# Combined spectroscopic and modeling study of trans-stilbene molecule in cation-exchanged ZSM-5 zeolites

Matthieu Hureau, Alain Moissette, Konstantin Smirnov, Hervé Jobic

# Combined Spectroscopic and Modeling Study of *trans*-Stilbene Molecule in Cation-Exchanged ZSM-5 Zeolites

Matthieu Hureau,[†] Alain Moissette,*[,†] Konstantin S. Smirnov,[†] and Hervé Jobic[‡]

[†]Laboratoire de Spectrochimie Infrarouge et Raman UMR-CNRS 8516, Bât. C5, Université de Lille 1, 59655 Villeneuve d'Ascq cedex, France

[‡]Institut de Recherches sur la Catalyse et l'Environnement de Lyon UMR-CNRS 5256, 2 avenue Albert Einstein, 69626 Villeurbanne cedex, France

ABSTRACT: A variety of spectroscopic methods and molecular modeling were used to characterize trans-stilbene (t-St) molecules sorbed in aluminum rich M-ZSM-5 zeolites (M+ =Na+,K+,Rb+,Cs+). The Monte Carlo simulations followed by the energy minimization predict the t-St sorption in the straight channels in close proximity of the extra-framework M+ ions. The effects of the interactions between the guest molecules and host zeolite lattice on the electronic states are examined experimentally by the diffuse reflectance UV−visible absorption and fluorescence emission, whereas the vibrational states are studied by means of Raman scattering, infrared absorption, and inelastic neutron scattering techniques. The changes observed in the spectra are found to depend on type of charge-balancing cation and to intensify with the increase in cation size. Comparison of experimental data and results of quantum-chemical calculations allows explaining the features observed in the Raman spectra of the systems. Results of the study lead to the conclusion that the properties of occluded t-St molecules are mainly governed by molecule−cation interactions, whereas the confinement by zeolite lattice imposes sterical hindrances on the possible conformations of t-St/cation complexes.

## INTRODUCTION

The incorporation of molecules into the internal void of microporous materials allows studying the chemical and photochemical properties of individual molecules and permits us to control the chemical processes by a judicious choice of size and shape of the confining space. Among such materials, zeolites are of particular interest because they are characterized by a regular porous structure and offer a wide range of framework topologies. Zeolites are crystalline aluminosilicates of general formula $|M^+_n|[Al_nSi_mO_{2(m+n)}]^{n-}$ in which the substitution of Si(IV) by Al (III) atom in the lattice requires the presence of charge-balancing cations $M^+$ to ensure the charge neutrality. High specific surface area, accessibility of extra-framework cations, and shape selectivity of crystalline lattice with respect to sorbed molecules have led to many industrial applications of zeolites such as acid catalysts in oil chemistry, in ion exchangers, and in gas separation.[1−5] Medium pore size ZSM-5 zeolites (MFI structure type) have a porous system consisting of intersecting channels of two types formed by rings of ten oxygen atoms. Channels called straight channels run along the *b* crystallographic axis and have a nearly circular shape of 0.53 nm × 0.56 nm, whereas the second type of channels, sinusoidal channels, have an average direction along the *a* axis with an opening of 0.51 nm × 0.55 nm. Molecules of size smaller than the pore dimension are able to diffuse in the porous system, but the particular shape of sinusoidal channels results in a slower diffusion of even small molecules in these channels than in straight ones. Furthermore, the presence of extra-framework cations in the void can strongly affect the behavior of guest species. Recently, we reported the remarkable influence of the cation nature on the reactivity of electron donor molecules sorbed in M-ZSM-5 zeolites ($M^+$ = $H^+$, $Li^+$, $Na^+$, $K^+$, $Rb^+$, $Cs^+$). For this structure, the interactions of polyaromatic hydrocarbon and diphenyl-polyene molecules with the atoms of host lattice and with the charge-balancing cations were found to be responsible for ionization of the guest molecules and resulted in the formation of long-lived charge-separated states.[6−9] The nature of the cation was found to affect drastically the electron donor ability of the zeolite framework and plays a crucial role for the stabilization of charge-separated states.[10,11]

Molecules of diphenyl-polyene family and *trans*-stilbene (*t*-St), in particular, are of significant interest for the chemistry, photophysics, and material science. *trans*-Stilbene is often considered as a prototype system for the photoisomerization reaction and as a model photosensitized electron-donor structure.[12−16] Consequently, there exists a large body of both experimental and computational studies aimed at elucidation of the structure of the molecule and its change upon photoexcitation. Results of X-ray analysis of the

molecule[17,18] in the solid phase and a number of computational studies[19] showed that the molecule has a planar conformation in the ground state and is characterized by the $C_{2h}$ symmetry point group.[20] Gas-phase electron diffraction data[21] and some computational studies[19] indicated that the two benzene rings are tilted with respect to the central C═C double bond. Recent experimental[22] and subsequent computational[23] studies have shown that encapsulation of *t*-St in organic hosts strongly influences the fluorescence properties of the molecule and that the size of the cage plays a crucial role by allowing the molecule to accept specific conformation in both the ground and excited states.

The size of phenyl group of ca. 0.5 nm and the alignment of the groups in the *trans*-stilbene isomer makes the molecule a good probe for investigation of possible changes in its structural and electronic properties upon interaction with an inorganic matrix. In particular, the size of the molecule allows it to be included into the channel system of ZSM-5 zeolite. The structure of the *t*-St/ZSM-5 complex has been previously investigated using synchrotron X-ray scattering technique.[24,25] This study demonstrated that *t*-St sorption occurred in a straight channel with one phenyl ring close to the intersection of the straight and sinusoidal channels. The sorption of two molecules per unit cell was found to produce an elliptical distortion of the shape of straight channels of the framework.

The present article reports results of combined experimental and modeling study of *t*-stilbene molecule occluded in cation-exchanged M-ZSM5 zeolites (M = $Na^+$, $K^+$, $Rb^+$, $Cs^+$). The systems were characterized by a variety of spectroscopic methods. The electronic states were examined by the diffuse reflectance UV−vis absorption (DRUVv) spectroscopy and emission fluorescence techniques. The vibrational dynamics of the *t*-St/zeolite systems was studied by means of the Raman scattering, infrared absorption, and inelastic neutron scattering methods.

The experimental data obtained by these techniques were completed by results of molecular modeling. The sorption sites and the conformations of occluded *t*-St molecules were investigated by the Monte Carlo (MC) and energy minimization (EM) calculations. The interpretation of the vibrational spectroscopic results was carried out on the basis of ab initio calculations of both a free molecule and *t*-St complexes with $Na^+$, $K^+$, and $Cs^+$ ions. The presented results complete the structural data of refs 24 and 25 and are expected to assist the interpretation of our recent studies on the (photo)chemistry of *t*-St in ZSM-5 zeolites.[10,11]

## EXPERIMENTAL SECTION

**Characterization of Exchanged Zeolites.** As-synthesized ZSM-5 samples (Si/Al = 13.5; average particle size ∼1 $\mu$m) were obtained according to the template procedure in alkaline medium from VAW aluminum (Schwandorf, Germany). The as-synthesized zeolite structures were calcined at 450 °C under air to evacuate the template. The initial $Na^+$ extra-framework cation of aluminated zeolites was exchanged by $Li^+$, $K^+$, $Rb^+$, or $Cs^+$ using the corresponding MCl salts. The exchange process was carried out by suspending the zeolite sample in MCl aqueous solution under stirring. After 24 h, the solid phase was filtered off and dried at 200 °C in oven for 12 h, then stirred again with a fresh solution of the chloride salt and then dried. The procedure was repeated four times. The resulting sample was washed by deionized water, isolated, dried at 200 °C for 12 h, and then calcined at 450 °C in ambient air for 6 h. The elementary analyses of the M-ZSM-5 samples indicated that the $Na^+$ cations of the parent material have been completely exchanged by $Li^+$, $K^+$, $Rb^+$, or $Cs^+$ using the above procedure. The unit cell analyses of M-ZSM-5 samples yielded the $M_{6.6}(AlO_2)_{6.6}(SiO_2)_{89.4}$ formula. The chemical analyses, powder XRD patterns, $^{29}Si$, $^{27}Al$ MAS NMR, IR, Raman, DRUVv, and EPR spectra of bare exchanged zeolites were found to be characteristic of diamagnetic well-crystallized porous compounds. However, the $^{27}Al$ MAS NMR spectra of hydrated M-ZSM-5 provided evidence of the presence of small amount of extra-framework hexacoordinated aluminum species.

**Preparation of *t*-St Loaded Zeolites.** Weighed amounts (∼1.4 g) of exchanged zeolite sample were introduced to an evacuable heatable silica cell placed in a vertical oven connected to a piping network. The sample was heated stepwise up to 450 °C under the flow of dry argon for 3 h, and the sample was then cooled to room temperature in the argon atmosphere. Weighed amounts of *t*-St corresponding to one molecule per unit cell of M-ZSM-5 were introduced to the cell under dry Ar; then, the powder mixture was shaken. After homogeneous mixing, the powder was transferred under dry argon to a quartz glass Suprasil cell and sealed. All *t*-St@M-ZSM-5 samples were stocked in the sealed cells at 40 °C for 6 months in the dark. The inter- and intracrystalline migrations of *t*-St molecules were monitored by the conventional diffuse reflectance UV−visible absorption spectroscopy and Raman spectroscopy. After six months, the *t*-St loaded samples exhibit the UV absorption and Raman bands characteristic of *t*-St occluded in molecular form without any spontaneous ionization, as observed in acidic H-ZSM-5. However, a weak amount of *t*-stilbene radical cation species was observed in Li-ZSM-5 structure. Consequently, this sample was excluded from the consideration in the present study.

## INSTRUMENTATION

**Diffuse Reflectance UV−Visible (DRUVv) Absorption Spectroscopy.** The UV−visible absorption spectra of the samples in the ground state were recorded in the region 200−900 nm using a Cary 6000 spectrometer. The instrument was equipped with an integrating sphere to study the diffuse reflectance of powdered *t*-St/zeolite samples stocked under an inert atmosphere in quartz cells; the corresponding bare zeolite was used as the reference. The DRUVv spectra were plotted as the Kubelka−Munk function

$$F(R) = (1 - R)^2/2R = K/S \quad (1)$$

where $R$ represents the ratio of the diffuse reflectance of the loaded zeolite to that of the dehydrated neat zeolite, $K$ designates an absorption coefficient proportional to the concentration of molecule, and $S$ is the scattering coefficient of the powder.

**DRIFTS.** The FTIR instrument is a Nicolet Magna 860 apparatus equipped with a liquid-nitrogen-cooled MCT detector (Mid-IR) with the suitable beam splitter. The spectra were recorded with a 2 $cm^{-1}$ resolution using 1064 scans.

**Raman Spectroscopy.** A Bruker RFS 100/S instrument was used as a near-IR FT-Raman spectrometer with a CW Nd:YAG laser ($\lambda_0$ = 1064 nm) as excitation source. A laser power of 100−200 mW was used. The spectra of samples stocked under argon in the quartz cells were recorded in the region 3500−150 $cm^{-1}$ with a 2 $cm^{-1}$ resolution using 600 scans.

**Fluorescence Emission.** The experiments were carried out on a Fluoromax 3 (Jobin Yvon) spectrometer using a xenon lamp (150 W) as excitation source.

**Inelastic Neutron Scattering.** The inelastic neutron scattering (INS) experiments were performed on the IN1BeF spectrometer at the Institut Laue-Langevin (ILL) in Grenoble, France. IN1BeF is a beryllium filter detector spectrometer using neutrons delivered from the hot source of the ILL. The incident energy on this spectrometer is varied stepwise and is selected by Bragg scattering from different copper monochromators. In this work, the target energy range was covered with the Cu(220) plane. This configuration gives a high flux, but a moderate instrumental resolution that varies from 3 meV (24.2 $cm^{-1}$) at low energy transfers to 6 meV (48.4 $cm^{-1}$) at large energy transfers. Only scattered neutrons, which have lost energy owing to a vibrational transition and which have a mean energy of ~3.7 meV (30 $cm^{-1}$) can pass through the beryllium filter before being detected. The spectra are thus shifted up in energy by this value, but the frequency values given in the text have been corrected for this effect. The estimated accuracy on the frequency values is ca. 2.5 meV (20 $cm^{-1}$). The spectra were recorded at 10 K to decrease the mean-square amplitude of the atoms and thus to sharpen the vibrational peaks. The samples were contained in sealed cylindrical aluminum cells. The transfer of the equilibrated sample from the quartz cell to the neutron cell was carried out under an inert atmosphere in a glovebox. It is worth noting that the INS spectra are related to the density of vibrational states and show all possible vibrational transitions of the system. A discrimination of the vibrational modes over the symmetry can be done by using the infrared and Raman experiments.

## COMPUTATIONS

**Structural Models.** The modeling of *trans*-stilbene sorption in the M-ZSM-5 zeolites was performed with Material Studio Modeling package (version 5.2) from Accelrys International. The positions of atoms in zeolite framework were taken from the results of X-ray and neutron diffraction studies.[26,27] The substitution of Si by Al atoms in the framework was done in T-atom sites of immediate vicinity of location of the $Cs^+$ ions in Cs-exchanged ZSM-5 zeolite determined in XRD experiments.[28,29] The positions of extra-framework cations were then optimized by MC simulations and kept fixed in the modeling of *t*-St sorption (vide infra). The structure of the *t*-St molecule was taken from previous works.[30]

**Force Fields.** The zeolite-sorbate interaction energy $E_{ZS}$ was described by the sum of Lennard-Jones (LJ-9-6) and Coulombic potentials

$$E_{ZS} = \sum_{ij} A_{\alpha\beta}/r_{ij}^{9} - B_{\alpha\beta}/r_{ij}^{6} + q_i q_j / r_{ij} \quad (2)$$

where the indices $i$ and $j$ run over atoms of the zeolite and of the guest molecule, respectively, and the indices $\alpha$ and $\beta$ stand for the atomic kinds of the atoms $i$ and $j$. Values of the $A_{\alpha\beta}$ and $B_{\alpha\beta}$ parameters for unlike interactions were obtained by Waldman–Hagler combination rules[31] with the help of the $A_{\alpha\alpha}$ and $B_{\beta\beta}$ like parameters for the H, C, and O atoms and $Na^+$, $K^+$, $Rb^+$, and $Cs^+$ ions of the COMPASS force field.[32] In the calculation of the host–guest interaction energy, the Lennard-Jones interactions of "buried" Si and Al atoms with extra-framework cations and with atoms of guest molecule were omitted. The partial charges $q_i$ of Si, Al, and O atoms of zeolite lattice and of $M^+$ ions were the same as those used in refs 28 and 29. The charges of atoms of *t*-St molecule were taken from results of ab initio calculations of the molecule.[30] The intramolecular energy $E_S$ of *t*-St molecule was described with a molecular mechanics force field

$$E_S = \Sigma_{bonds} K_r (r - r_0)^2 + \Sigma_{angles} K_\theta (\theta - \theta_0)^2 + \Sigma_{dihedral} K_\phi [1 + \cos(\phi n - \gamma_0)] \quad (3)$$

where $K_r$, $K_\theta$, and $K_\phi$ are the force constants for bond-stretching, angle-bending, and torsional internal coordinates, respectively, and $r_0$, $\theta_0$, and $\gamma_0$ are the equilibrium bond lengths, valence angles, and torsional angles in a free *t*-St molecule. Values of the parameters of eq 3 were taken from the COMPASS force field.[32]

**Monte Carlo Simulations.** The preferred adsorption sites of *t*-St molecule in the M-ZSM-5 zeolites were obtained in MC simulations using the Metropolis algorithm for the canonical *NVT* statistical ensemble. The calculations were performed for the temperature of 298 K. The simulation box consisted of 2 × 2 × 4 orthorhombic cells of zeolite lattice and of one guest molecule; the periodic boundary conditions were applied to the system in all directions. A cutoff radius of 1.2 nm was used for the L-J potential, whereas the long-range electrostatic interactions were treated with the Ewald sum method. In the MC simulations, the positions of framework atoms and of charge-balancing cations were fixed, and the structure of *t*-St molecule was kept rigid. One MC step consisted of a random displacement or of an arbitrary rotation of the molecule as a whole.

The docking procedure preceding each MC simulation always found the position of molecule in a straight channel to be much more energetically preferred over a location of *t*-St in a sinusoidal channel, in agreement with the experimental data.[24,25] The initial configuration of MC simulations therefore corresponded to *trans*-stilbene situated in a straight channel of zeolite structure. A typical MC simulation run took $10^8$ steps, and the first $10^6$ steps corresponding to the equilibration period were excluded from the subsequent analysis. A histogram of the $E_{ZS}$ energy distribution was generated in each simulation run. For each studied system, the configuration with the minimum energy was used in EM calculations aimed at the optimization of the structure of cation–molecule complex in the zeolite void.

**Energy Minimization Calculations.** In the EM calculations, the zeolite framework was held rigid, whereas the charge-balancing cations and atoms of *t*-St molecule were allowed to move. The total energy of the system was described by the sum of $E_{ZS}$ and $E_S$ energies (eqs 2 and 3). The EM was performed using the conjugate gradient minimization algorithm.

**Calculation of the Vibrational Spectra.** The vibrational analysis of a free *t*-St molecule and of $M^+$-*t*-St complexes ($M^+$ = $Na^+$, $K^+$, $Cs^+$) was performed with the help of ab initio quantum-chemical calculations using Gaussian03 code.[33] The calculations were carried out at the DFT level with the B3LYP exchange-correlation functional and 6-311(d,p) basis set for H, C, Na, and K. The LANL2DZ effective core potential was used for the Cs atom. The geometry optimization of a free *t*-St molecule was done assuming either the planar geometry of the molecule ($C_{2h}$ point group) or without any symmetry constraints in the $C_1$ symmetry.

Results of ref 19 showed that the structure of *t*-stilbene molecule is sensitive to the level of theory used in quantum-

chemical calculations. Consequently, in addition to the DFT calculations, the geometry optimization, followed by the vibrational analysis, was carried out for a free *t*-stilbene molecule at the MP2 level using the same 6-311(d,p) basis set. The MP2 calculations were done for both the $C_{2h}$ and $C_1$ conformations.

The computation of the infrared absorption coefficients and Raman scattering activities of vibrational modes for the optimized structures was done via the internal capabilities of the Gaussian03 code. To be compared with the intensity in the experimental Raman spectra, the Raman scattering activity of mode $k$ was scaled by the factor (assuming Stokes scattering)

$$S(\omega_k, T) = (\omega_0 - \omega_k)^4/\omega_k(1 - \exp(-\omega_k/k_B T)) \qquad (4)$$

where $\omega_k$ is the frequency of the mode, $\omega_0$ stands for the frequency of the exciting radiation, and $k_B$ and $T$ are the Boltzmann constant and temperature, respectively. The spectrum was then convoluted with a Lorentzian function with the hwhm equal to 4 $cm^{-1}$. The Raman spectra calculations did not take the zeolite lattice into account because the perturbations of molecular vibrational states by weak interactions with the solid were expected to be small. Furthermore, the calculation of Raman scattering intensities of complete *t*-St/zeolite system would simply be unfeasible with the present methodology. A posteriori justification of this assumption is reported in the following section of the article.

The INS spectra were simulated following previous works.[34−36] The vectors of Cartesian atomic displacements in vibrational modes were obtained from the eigen-vectors of mass-weighted Hessian matrix taken from the Gaussian03 checkpoint file. The INS intensities were computed assuming the one-phonon scattering mechanism and in the isolated-molecule approximation. The influence of the zeolite lattice on the INS spectra was taken into account in an indirect way by considering the contribution of external zeolite modes into the two-phonon scattering. The frequency of the bath mode used for these calculations was equal to 100 $cm^{-1}$, which approximately corresponds to the frequency of breathing vibrations of zeolite pore system.[37,38] The calculations showed that the two-phonon scattering due to both the internal and external modes has a small contribution to the total scattering intensity. To be compared with the experimental INS spectra, the computed scattering intensities were convoluted with a Gaussian function having hwhm of 2 meV (ca. 16 $cm^{-1}$) corresponding to the experimental resolution.

## RESULTS AND DISCUSSION

**1. *t*-St Sorption in M-ZSM-5 Zeolites.** Figure 1 shows *t*-St molecule sorbed in Na-ZSM-5-zeolite and illustrates a situation typical of the minimum energy conformation of the *t*-St@M-ZSM-5 complexes. The molecule lies in a straight channel with two phenyl rings situated in the intersections of the straight and sinusoidal channels of the zeolite lattice. One of the phenyl rings is facially coordinated to the $M^+$ cation by cation−$\pi$ interaction. The EM allowing for the flexibility of *t*-St structure and the mobility $M^+$ ions resulted only in small displacements of the entities with respect to the positions obtained in the MC simulations. Table 1 gathers some geometrical characteristics obtained in the MC/EM calculations for *t*-St/cation complexes in zeolites and in ab initio calculations for free complexes. One sees that the distance between the cation and the plane of phenyl ring increases with the increase in the cation radius in both the occluded and free complexes. The differences in the distances obtained for the occluded and free *t*-St/cation complexes are obviously due to the sterical hindrances imposed by the zeolite lattice on possible complex conformations in the zeolite void. The structure of molecule after the EM shows a deviation from the planar geometry. It is noteworthy that the sorbed molecule is characterized by a larger tilting angle $\phi$ than in free *t*-St/M complexes. The DFT calculation of a free *t*-St in which the constraint of planar structure in the geometry optimization was relaxed leads to the tilt angle of 9.6° between the two phenyl rings of the molecule. Such a configuration is more energetically stable than the planar structure of $C_{2h}$ symmetry by only $2 \times 10^{-3}$ kcal/mol. The MP2 calculation of a free molecule in $C_1$ symmetry gives the tilt angle of 53.8° and the energy difference of $-7 \times 10^{-2}$ kcal/mol with respect to the planar molecular structure; the tilted conformation was found to be more stable that the $C_{2h}$ one. These results are in agreement with data of quantum-chemical calculations[19] that pointed to a small energy difference between the planar and tilted conformations of *trans*-stilbene. The authors of ref 19 suggested that the planar conformation of *t*-St molecule in solution and in solid state is due to the intermolecular interactions.

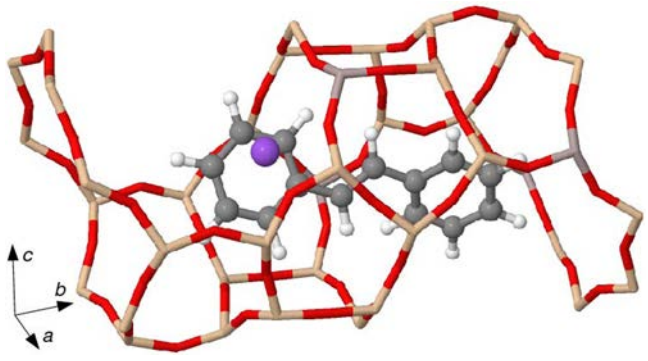


**Figure 1.** *t*-St-predicted sorption site in straight channel of NaZSM-5. Red, yellow, and gray sticks represent the O, Si, and Al atoms of the framework, respectively. The white and shaded spheres represent the H and C atoms of the *t*-stilbene molecule, respectively. The puple sphere represents the $Na^+$ cation.

The distribution of $E_{ZS}$ energy obtained for *t*-St occluded in M-ZSM-5 zeolites is presented in Figure 2. The mean values of the host−guest interaction energy weakly depend on the cation type and were found to slightly increase from $Na^+$ to $Cs^+$ (Table 1). The energy distributions are characterized by a relatively small width ($\approx$ 2 kcal $mol^{-1}$) that implies the existence of only one *t*-St sorption site for each system in agreement with the XRD data by Parise et al.[24,25] The repartition of the energy into the van der Waals and electrostatic contributions indicates the major role of the van der Waals interactions whose variations account for the changes of the total energy. Only a weak variation of the electrostatic energy term as a function of charge-compensating cation can be observed. The molecular modeling results therefore point to the major role of the zeolitic framework and of van der Waals interactions for the conformation of the sorbed *t*-St molecule.

The DFT calculations of free *t*-St/cation complexes yield the interaction energy between the molecule and cation equal to −29.2 kcal/mol ($Na^+$), −20.5 kcal/mol ($K^+$), and −12.0 kcal/mol ($Cs^+$). The general tendency of the interaction energy is in a line with the trend found in the classical simulations. It should

**Table 1. Characteristics of *t*-St/M Complex Obtained in MC/EM Calculations for *trans*-Stilbene Occluded in M-ZSM-5 Zeolites and in DFT Calculations for a Free *t*-St/$M^+$ Complex[a]**

| $M^+$ | *t*-St@M-ZSM-5 | | | | free *t*-St/complex | | | |
|---|---|---|---|---|---|---|---|---|
| | $E_I$ (kcal $mol^{-1}$) | $R_{M\text{-}Ph}$ (Å) | $R_{M\text{-}C}$ (Å) | $\phi$ (deg) | $E_I$ (kcal $mol^{-1}$) | $R_{M\text{-}Ph}$ (Å) | $R_{M\text{-}C}$ (Å) | $\phi$ (deg) |
| $Na^+$ | −29.6 | 2.38 | 2.53 | 45.4 | −29.2 | 2.37 | 2.74 | 0.2 |
| $K^+$ | −27.4 | 2.94 | 2.94 | 17.6 | −20.5 | 2.82 | 3.12 | 6.6 |
| $Rb^+$ | −26.0 | 3.06 | 3.06 | 18.2 | | | | |
| $Cs^+$ | −25.5 | 3.77 | 3.86 | 18.8 | −12.0 | 3.45 | 3.62 | 5.9 |

[a] $E_I$, sorption energy and molecule-cation interaction energy for sorbed molecule or *t*-St/$M^+$ complex, respectively; $R_{M\text{-}Ph}$, distance from the cation $M^+$ to the plane of phenyl ring; $R_{M\text{-}C}$, distance from the cation $M^+$ to the closest carbon atom of the molecule; $\phi$, dihedral angle between the planes of two phenyl rings.

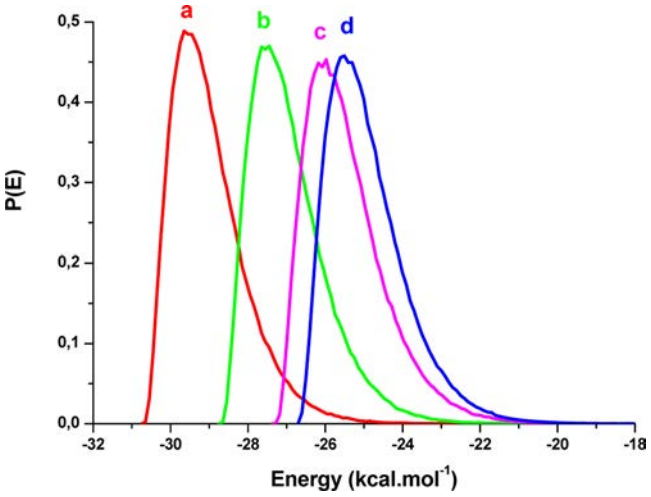


**Figure 2.** Distribution of calculated energies of *t*-St occluded in MZSM-5 zeolite at 298 K for the loading of one *t*-St molecule per unit cell: (a) $M^+ = Na^+$, (b) $M^+ = K^+$, (c) $M^+ = Rb^+$, and (d) $M^+ = Cs^+$.

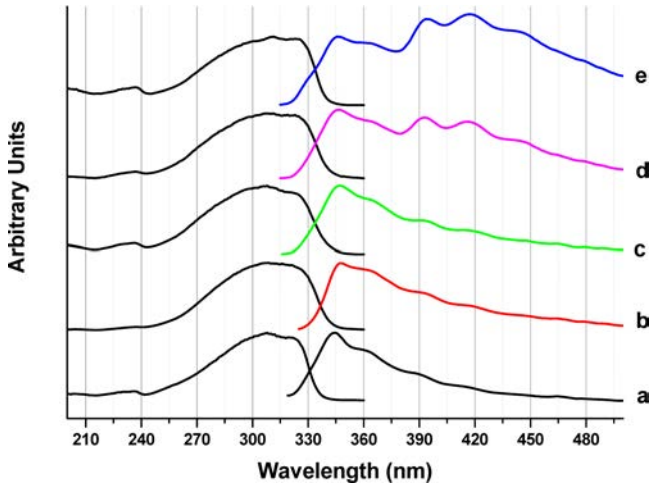


**Figure 3.** Diffuse reflectance UV−visible absorption (left) and fluorescence emission (right) spectra recorded 6 months after the mixing of solid *t*-St and $M_{6.6}$ZSM-5 dehydrated at 723 K under argon: (a) solid *t*-St, (b) $M^+ = Na^+$, (c) $M^+ = K^+$, (d) $M^+ = Rb^+$, and (e) $M^+ = Cs^+$.

be noted that the interaction energy computed for *t*-St/$Cs^+$ cation complex is probably underestimated because of an incomplete treatment of the dispersion interactions between the $\pi$-electrons of phenyl ring and highly polarizable $Cs^+$ cation in the DFT calculations.

**2. Diffuse Reflectance UV−Visible and Fluorescence Emission Spectroscopy.** The diffuse reflectance UV−visible (DRUVv) spectra obtained 6 months after the mixing of *t*-St and dehydrated M-ZSM-5 zeolites are presented in Figure 3. All spectra show an intense and broad absorption band in the UV region between 250 and 350 nm with a maximum at ∼310 nm. This absorption band is characteristic of the *t*-St molecule in the neutral form.[39] Note that even if weak shifts are observed for the maximum of intensity as a function of the cation type then no obvious tendency can be deduced from the spectra. In contrast, the fluorescence emission spectra recorded 6 months after mixing clearly show various behaviors according to the cation nature (Figure 3). The spectra obtained after an excitation performed at 300 nm show a broad band between 330 and 450 nm with a maximum at 345 nm for all samples. For *t*-St incorporated in Na-ZSM-5, weak bands are also observed at 366, 389, and 415 nm (Table 2). This spectrum is similar to the spectrum obtained in a polar solvent such as ethanol.[40,41] These spectral features are probably due to the vibronic transitions given that the distances between these maxima are equal to ∼1600 $cm^{-1}$ that roughly corresponds to the vibrational frequency of double CC bond. This finding suggests that the observed feature might be due to the vibrational dynamics of the molecule in the ground state. Note that no such a pattern could be observed in the excited state using the DRUVv absorption technique. The emission spectrum recorded for *t*-St occluded within K-ZSM-5 is very similar to that observed for Na-ZSM-5. Furthermore, in the structures exchanged with the bigger $Rb^+$ and especially $Cs^+$, the emission spectra show clearly the high intensity increase in the bands centered at 393, 416, and 445 nm with respect to those observed at 345 and 367 nm (Table 2).

**Table 2. Optical DRUVv, Fluorescence Emission and Raman Data for *t*-St Occluded in M-ZSM-5 ($M^+ = Na^+$; $K^+$, $Rb^+$, $Cs^+$) Dehydrated at 723 K under Argon**

| zeolite (Si/Al = 13.5) | $\lambda_{max}$ (nm) absorption | $\lambda_{max}$ (nm) emission | $\nu$ ($cm^{-1}$) Raman |
|---|---|---|---|
| Na-ZSM-5 | 308 | 345, 366, 389, 415 | 1637, 1602[a], 1594, 1192, 998, 963 |
| K-ZSM-5 | 309 | 346, 367, 390, 416 | 1639, 1602, 1593, 1192, 999, 963 |
| Rb-ZSM-5 | 309 | 345, 369, 393, 416, 444 | 1640, 1603, 1593, 1191, 999, 963 |
| Cs-ZSM-5 | 309 | 345, 367, 390, 415, 445 | 1640, 1603, 1593, 1190, 999, 963 |

[a] Shoulder.

**3. Vibrational Spectroscopy.** The Raman and IR spectra of *trans*-stilbene molecule in the solid phase and in solution are well-documented,[20,42−44] and the spectra do not significantly differ from each other. For the molecule characterized by the $C_{2h}$ symmetry, 72 vibrational modes are distributed over the symmetry species in the following way: $25A_g + 11B_g + 12A_u + 24B_u$, with the Raman active $A_g$ and $B_g$ modes inactive in the infrared spectrum and vice versa. Displacements of atoms in the $A_g$ and $B_u$ modes lie in the molecular plane, whereas the $B_g$ and $A_u$ modes correspond to the out-of-plane vibrations. There are no degenerate modes, and thus no splitting can be expected upon adsorption due to the lowering of symmetry. The complete assignment of the vibrational spectrum of *trans*-stilbene with $C_{2h}$ symmetry was done by Watanabe et al.[44] Results of the present DFT calculations of the IR and Raman intensities for the *t*-St molecule with nonplanar geometry show only a marginal violation of the selection rules specific to the planar structure with the $C_{2h}$ symmetry. Consequently, for the sake of clarity, the symmetry characters of vibrational modes of the molecule in the following discussion refer to those of the $C_{2h}$ point group.

*3.1. Inelastic Neutron Scattering.* Figure 4 shows the experimental INS spectra of *t*-St@Na-ZSM-5 and *t*-St@Cs-ZSM-5 systems and compares them with the simulated INS spectra of *t*-St@$Na^+$ and *t*-St@$Cs^+$ complexes and with the spectrum calculated for a free *trans*-stilbene molecule. The experimental spectra are well-reproduced by the simulated spectra of *t*-St/cation complexes, and they are very similar to the INS spectrum computed for an isolated molecule. This result justifies the use of the isolated molecule approximation in the simulation of the INS spectra. The analysis of Figure 4 reveals that the spectra of the zeolitic systems do not significantly differ from each other and small changes in intensities of some peaks can hardly provide any valuable information. This observation allows us to conclude that the interaction of molecule with the host structures only slightly perturbs the energies of molecular vibrational states and the forms of the vibrational modes. The analysis of vibrational modes shows that the most intense peaks at 1016 and 1202 $cm^{-1}$ are due to a number of close-lying modes that can be described as ring-breathing vibrations and in-plane CCH angle-bending vibrations, respectively.

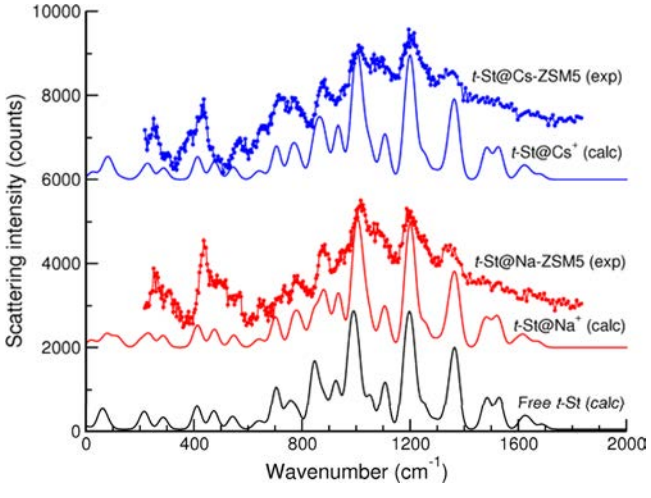


**Figure 4.** Experimental (exp) and simulated (calc) inelastic neutron scattering (INS) spectra of *t*-St@Na-ZSM-5 and *t*-St@$Na^+$ (red) and *t*-St@Cs-ZSM-5 and *t*-St@$Cs^+$ (blue). The simulated INS spectrum of free *t*-St molecule (black) is shown as a reference. The theoretical spectra are based on the results of the DFT calculations.

*3.2. Diffuse Reflectance Infrared Fourier Transform Spectroscopy (DRIFTS).* To get a better understanding of the behavior of occluded *t*-St molecules, the samples were also analyzed using DRIFTS technique. Figure 5 shows the spectra obtained for the equilibrated *t*-St@M-ZSM-5 systems (M = $Na^+$ and $Cs^+$). The spectra of a bare zeolite structure and of a solid *t*-stilbene are also presented for comparison. Unfortunately, too high intensity of zeolite bands with respect to weak *t*-St molecule signals does not permit us to extract the spectrum of occluded *trans*-stilbene by subtracting the zeolite contribution. The spectral region from 800 to 1400 $cm^{-1}$ is completely masked by the absorption of zeolite lattice modes,[45] and the broad and intense band centered at 1630 $cm^{-1}$ is due to an overtone of T-O symmetric stretching framework vibrations.[46] In the spectral region above 1400 $cm^{-1}$, the spectra of the *t*-St/zeolitic systems contain weak bands at ca. 1597 and 1584 $cm^{-1}$ (C−C stretching vibrations in phenyl rings), at 1498 and 1455 $cm^{-1}$ (in-plane CCH angle-bendings), and at 766 and 695 $cm^{-1}$ (ring puckering and out-of-plane CH bending vibrations).[42,44] The positions of bands in the IR spectrum of the *t*-St/zeolite systems differ from the positions in the spectrum of solid *trans*-stilbene by 6 $cm^{-1}$ at most, which suggests only a weak perturbation of the molecular vibrational states by the sorption.

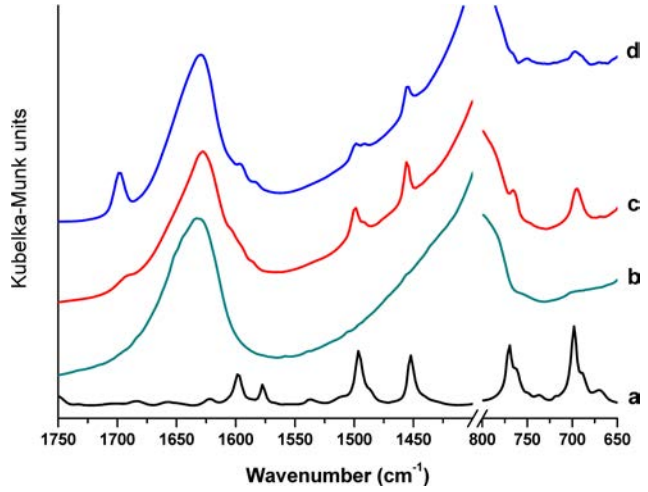


**Figure 5.** Diffuse reflectance infrared fourier transform (DRIFT) spectra of solid *t*-St (a), bare dehydrated Na-ZSM-5 sample (b), equilibrated *t*-St@Na-ZSM-5 (c), and *t*-St@Cs-ZSM-5 (d) samples.

The most notable change in the DRIFT spectrum is the appearance of a new band at 1700 $cm^{-1}$ for the *t*-St@Cs-ZSM-5 sample. This feature, which was never previously described, is also observed as a shoulder in the spectrum of *t*-St@Na-ZSM-5 system (Figure 5c). One might attempt to assign the band to one of molecular modes. However, the Raman peak at 1640 $cm^{-1}$ corresponds to the most high-frequency mode of the molecule in this spectral region (vide infra). Furthermore, all INS data suggest a weak perturbation of the molecular vibrations by the host−guest interactions. In addition, the positions of infrared bands of occluded *t*-St show frequency shifts of only a few wavenumbers, whereas the position of the band at 1700 $cm^{-1}$, being assigned to a molecular vibrational mode, implies a shift of a few tens of wavenumbers, which is much more than the shifts measured for other vibrational

modes. Hence, the band cannot be attributed to a fundamental vibration of sorbed molecule. The high intensity of the band at 1700 $cm^{-1}$ compared with the intensities of bands at 1597 and 1455 $cm^{-1}$ does not allow assigning this feature to an overtone transition. The Fermi resonance effect also cannot explain the appearance of the band because no important downward shift, which could be induced by the resonance interaction, was observed for *trans*-stilbene modes in the region 1700−1400 $cm^{-1}$. Therefore, the unambiguous interpretation of this feature necessitates additional studies.

*3.3. Raman Spectroscopy.* Figure 6 displays the off-resonance Raman spectra of *t*-St@M-ZSM-5 samples and

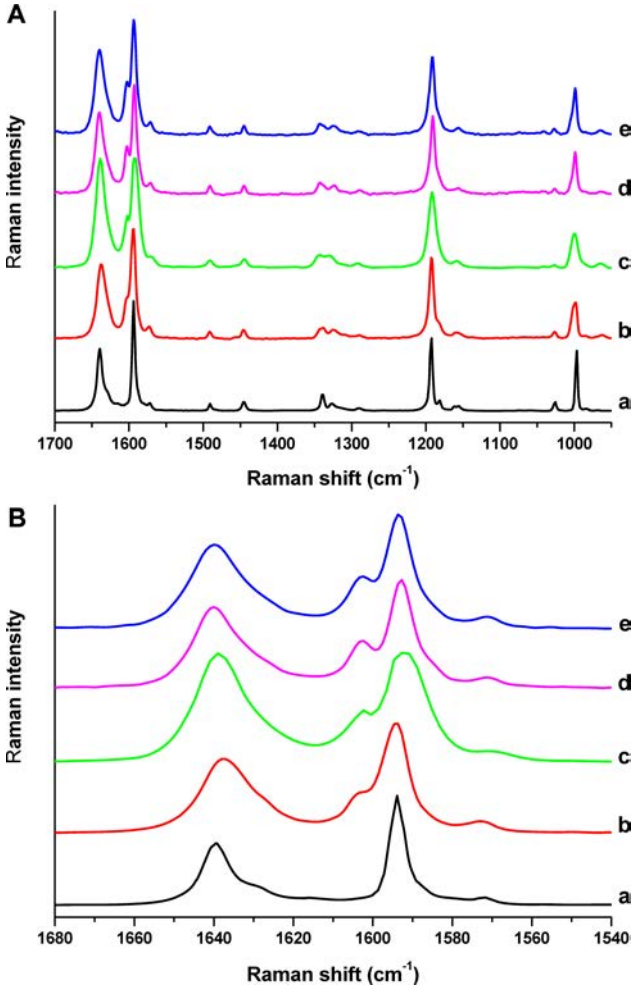


**Figure 6.** FT Raman ($\lambda$ = 1064 nm) spectra recorded for equilibrated *t*-St@$M_{6.6}$ZSM-5 dehydrated at 723 K under argon: (a) solid *t*-St, (b) $M^+ = Na^+$, (c) $M^+ = K^+$, (d) $M^+ = Rb^+$, and (e) $M^+ = Cs^+$. (A) In the 1700 to 950 $cm^{-1}$ spectral range. (B) In the 1680 to 1540 $cm^{-1}$ spectral range.

compares them with the Raman spectrum of *t*-St in solid phase (Figure 6a). The spectra are presented in the 900−1700 $cm^{-1}$ spectral range to highlight the interactions between the $M^+$ cations and the guest molecules through possible perturbations of the aromatic ring and central CC double bond vibrational modes. The spectra of *t*-St occluded in M-ZSM-5 zeolites are very similar to those of the molecule in the solid phase characterized by main Raman peaks at 1639 $cm^{-1}$ (stretching of central C═C bond), 1593 $cm^{-1}$ (CC stretching + CCH angle-bending), 1192 $cm^{-1}$ (CCC angle-bending in rings), and 996 $cm^{-1}$ (ring breathing).[43] Only small shifts and slight broadening of the peaks without notable changes in their relative intensities are observed upon the sorption. The spectral shifts are slightly sensitive to the nature of extra-framework cation. Therefore, the peak due to the stretching vibration of central C═C bond shifts from 1637 $cm^{-1}$ in Na-ZSM-5 to 1640 $cm^{-1}$ in Cs-ZSM-5. Besides these little changes, new Raman signals emerge upon *t*-St incorporation in the ZSM-5 channels. A new Raman peak is observed at 1603 $cm^{-1}$, which appears as a shoulder in the spectrum of *t*-St@Na-ZSM-5 system and rises in intensity with the increase in cation ionic radius from $Na^+$ to $Cs^+$ (Figure 6). Another low intensity band appears at 963 $cm^{-1}$ in the spectra of all samples.

Figure 7 shows the calculated Raman spectra of a free molecule and of *t*-St/cation complexes. The frequencies in the

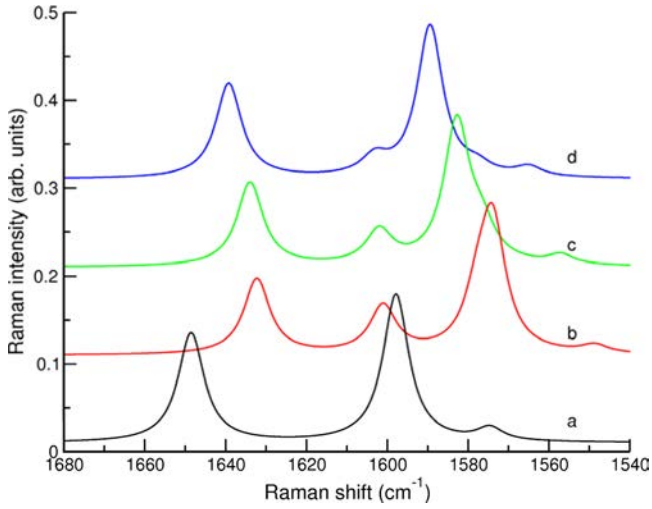


**Figure 7.** Computed Raman spectra of (a) free *t*-St molecule, (b) *t*-St@$Na^+$, (c) *t*-St@$K^+$, and (d) *t*-St@$Cs^+$ complexes. Results of DFT quantum-chemical calculations.

computed spectra were scaled by the factor 0.9776 obtained from the comparison of the vibrational frequencies computed for an isolated molecule with the experimental frequencies of *trans*-stilbene molecule in a solid state[44] in the spectral region 1000−1700 $cm^{-1}$. The interaction of the molecule with the cations leads to a downward shift of Raman peaks and to the appearance of a signal at 1601 $cm^{-1}$ close to the position of the Raman peak at 1603 $cm^{-1}$ coming up in the experimental spectra of zeolitic systems. The calculations show that this new Raman active mode arises from the $B_u$ mode at 1603 $cm^{-1}$ of a free *t*-St molecule that becomes Raman active in the stilbene−cation complexes. Displacements of atoms in the parent $B_u$ mode and in the 1601 $cm^{-1}$ Raman active mode of *t*-St@$Na^+$ complex are displayed in Figure 8. The computed Raman spectra of *t*-St/cation complexes also show the appearance of a Raman peak at 967 $cm^{-1}$ (not shown) that originates from the $A_u$ mode of isolated molecule at 969 $cm^{-1}$. The Raman activity of this formerly forbidden mode is in line with the appearance of the 963 $cm^{-1}$ peak in the experimental Raman spectra of sorbed molecules. This mode can be characterized as in-phase out-of-plane CH vibration of the CH═CH group. Displacements of atoms in the corresponding mode of the *t*-St@$Na^+$ complex are presented in Figure 9. Both the DFT and MP2 calculations of a free *trans*-stilbene molecule show that the Raman activity of this mode also arises from the twisting the

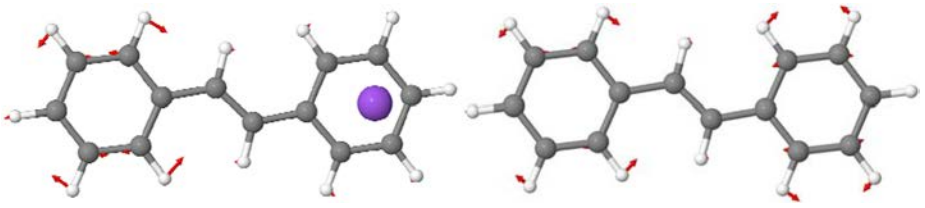

**Figure 8.** Atomic displacements in the 1603 $cm^{-1}$ vibrational mode of *t*-St@$Na^+$ complex (left) and in the parent $B_u$ mode of a free *trans*-stilbene molecule (right). Sodium ion is shown as a big purple ball. Results of DFT quantum-chemical calculations.

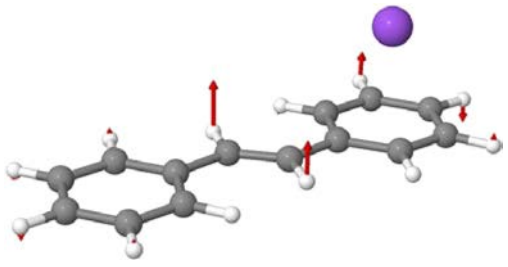

**Figure 9.** Atomic displacements in the 969 $cm^{-1}$ vibrational mode of *t*-St@$Na^+$ complex. Results of DFT quantum-chemical calculations.

two phenyl rings with respect to each other, whereas the intensity of modes in the region 1400−1700 $cm^{-1}$ is almost unaffected by the nonplanar structure of the molecule. It is noteworthy that no significant Raman intensity for other $B_u$ and $A_u$ modes was computed for the molecular structures with nonplanar geometry. This finding is in an agreement with the data of ref 19, where the planar and nonplanar configurations of *t*-St molecule were computed to have very similar spectra. Hence, the computational results allow explaining the observed Raman spectral features of the *t*-St@M-ZSM-5 systems in the region 1400−1700 $cm^{-1}$ as primarily due to the molecule−cation interaction, whereas the new Raman peak appearing in the spectra of occluded *t*-stilbene at 963 $cm^{-1}$ is due to both the nonplanar geometry of the molecules and the molecule−cation interaction.

Despite the fact that the DFT calculations permit us to account for the appearance of new peaks in the Raman spectra of the *t*-St@zeolite complexes, there exist two features that the calculations of free *t*-St/cation complexes do not mimic. First, the measured frequency shifts induced by the *t*-St/zeolite interactions are notably smaller than the shifts calculated for free complexes. Second, the experimental data suggest that the largest perturbation of the molecule occurs in Cs-exchanged ZSM-5 structure, whereas the DFT calculations indicate that the interaction of *t*-St molecule with cesium cation affects the vibrational dynamics of the molecule to a lesser extent. Indeed, taking the intensity of the 1603 $cm^{-1}$ Raman peak as a measure of the perturbation strength (Figure 6), one sees that the intensity is largest in the *t*-St@Cs-ZSM-5 system, in contrast with the quantum-chemical results showing the less perturbed molecule in the *t*-St@$Cs^+$ complex (Figure 7). It is worth noting that the results of MC calculations also show that the *t*-St molecule has a lower adsorption energy in Cs-ZSM-5 zeolite than in sodium one. These discrepancies can probably be attributed to the confinement effect. One can suppose that the molecule−cation interaction interferes with the cation−framework and molecule−framework interactions. Therefore, the cation−framework interactions bind the cations to specific extra-framework sites, and because the Na cations have smaller size than the Cs cations, one can expect that the former are closer to the zeolite walls as compared with the latter. Therefore, the small sodium ions are expected to be less accessible to the sorbed molecules because of the constraints imposed by the size and shape of zeolite void. These hindrances do not allow the molecule to approach the cation in a way to form a complex with the structure similar to that in a free state. This hypothesis is, however, not supported by the data of Table 1 that show that the characteristic distances between the molecule and $Na^+$ ion in both sorbed and free state do not significantly differ from each other. Simulations taking the framework flexibility into account and thus allowing for the distortion of the zeolite lattice upon *t*-stilbene sorption[24,25] are probably necessary to shed a light on the origin of the discrepancy.

## CONCLUSIONS

The results of experimental studies performed with a variety of spectroscopic techniques show that the *trans*-stilbene molecule is adsorbed in M-ZSM-5 zeolites (M = $Na^+$, $K^+$, $Rb^+$, $Cs^+$) in a molecular form. The UV−visible spectra of the systems do not reveal notable changes compared with solid phase and in solution. Furthermore, the comparison of the experimental and calculated INS spectra of *t*-St occluded in M-ZSM-5 structures shows that the experimental data are in a good agreement with the spectrum computed for both a free *trans*-stilbene molecule and *t*-St/cation complexes. These results point to weak perturbation of the electronic and vibrational states of the molecule upon sorption.

Molecular modeling calculations performed by MC method followed by the EM predict *t*-St sorption in the straight channels with aromatic phenyl ring facially coordinated to $M^+$ ion. The feasibility of such configurations is supported by the spectroscopic experiments through the observation of changes in the spectra that depend on the cation type. Therefore, the fluorescence emission spectra exhibit a vibronic structure that intensifies with the cation size. Furthermore, small peak shifts and peak broadening are observed in the Raman spectra of occluded molecules as a function of extra-framework cation. These spectral modifications are accompanied by the appearance of new peaks at 1603 and 963 $cm^{-1}$ that increase in intensity with the cation size from $Na^+$ to $Cs^+$. Ab initio quantum-chemical calculations performed on free *t*-St/cation complexes demonstrate that these new Raman peaks are due to formerly forbidden modes that become Raman-active because of polarization of the molecule by the cation−$\pi$ interaction. A deviation of molecule from planar configuration was found to play a secondary role for the Raman activity of the modes. It should, however, be noted that the calculations of free complexes do not take into account the confinement effect by zeolitic lattice, and this effect is suggested to account for some differences between experimental and computational results. Because of strong absorption bands of the zeolite lattice

vibrations, the IR spectra are less informative compared with the Raman data, and no unambiguous interpretation can be done for some features in the observed IR spectra.

The results of spectroscopic measurements supported by the data of calculations indicate that the zeolite framework acts as a chemically inert matrix that imposes sterical constraints on the possible molecular conformations and the dynamics of *trans*-stilbene molecules in the zeolite void. In the cation-exchanged zeolite structures, the characteristics of *t*-St molecules depend on the nature of charge-balancing cations, and, in contrast with free cation-molecule complexes, the stronger influence is found to be caused by cations of larger size.

## AUTHOR INFORMATION

### Notes

The authors declare no competing financial interest.

## ACKNOWLEDGMENTS

Neutron measurements were performed on IN1BeF at the Institut Laue-Langevin, Grenoble, France; we thank Dr. A. Ivanov for his help during the experiment.

## REFERENCES

(1) Garcia, H.; Roth, H. D. *Chem. Rev.* **2002**, *102*, 3947−4007.
(2) Vispute, T. P.; Zhang, H.; Sanna, A.; Xiao, R.; Huber, G. W. *Science* **2010**, *330*, 1222−1227.
(3) Rhodes, C. J. *Sci. Prog.* **2010**, *93*, 223−284.
(4) Park, H. J.; Heo, H. S.; Jeon, J. K.; Kim, J.; Ryoo, R.; Jeong, K. E.; Park, Y. K. *Appl. Catal., B* **2010**, *95*, 365−373.
(5) Huang, J.; Long, W.; Agrawal, P. K.; Jones, C. W. *J. Phys. Chem. C* **2009**, *113*, 16702−16710.
(6) Marquis, S.; Moissette, A.; Vezin, H.; Bremard, C. *C. R. Chim.* **2005**, *8*, 419−440.
(7) Moissette, A.; Lobo, R. F.; Vezin, H.; Al-Majnouni, K. A.; Bremard, C. *J. Phys. Chem. C* **2010**, *114*, 10280−10290.
(8) Vezin, H.; Moissette, A.; Hureau, M.; Bremard, C. *ChemPhysChem* **2006**, *7*, 2474−2477.
(9) Belhadj, F.; Moissette, A.; Bremard, C.; Hureau, M.; Derriche, Z. *ChemPhysChem* **2011**, *12*, 1378−1388.
(10) Hureau, M.; Moissette, A.; Vezin, H.; Bremard, C.; Orio, M. *J. Phys. Chem. C* **2012**, *116*, 1812−1825.
(11) Hureau, M.; Moissette, A.; Legrand, A.; Luchez, F.; Sliwa, M.; Bremard, C. *J. Phys. Chem. C* **2012**, *116*, 9092−9105.
(12) Lin, Y. D.; Chow, T. J. *J. Mater. Chem.* **2011**, *21*, 14907−14916.
(13) Lin, C. L.; Chen, C. H.; Lim, T. S.; Fann, W.; Luh, T. Y. *Chem. Asian J.* **2008**, *3*, 578−584.
(14) Ricks, A. B.; Solomon, G. C.; Colvin, M. T.; Scott, A. M.; Chen, K.; Ratner, M. A.; Wasielewski, M. R. *J. Am. Chem. Soc.* **2010**, *132*, 15427−15434.
(15) Rettig, W.; Strehmel, B.; Majenz, W. *Chem. Phys.* **1993**, *173*, 525−37.
(16) Porel, M.; Jockusch, S.; Parthasarathy, A; Rao, V. J.; Turro, N. J.; Ramamurthy, V. *Chem. Commun.* **2012**, *48*, 2710−2712.
(17) Bernstein, J. *Acta Crystallogr., B* **1975**, *31*, 1268−1271.
(18) Bouwstra, J. A.; Schouten, A.; Kroon, J. *Acta Crystallogr., C* **1984**, *40*, 428−431.
(19) Choi, C. H.; Kertesz, M. *J. Phys. Chem. A* **1997**, *101*, 3823−3831.
(20) Furuya, K.; Kawato, K.; Yokoyama, H.; Sakamoto, A.; Tasumi, M. *J. Phys. Chem. A* **2003**, *107*, 8251−8258.
(21) Traetteberg, M.; Frantsen, E. B.; Mijhlhoff, F. C.; Hoekstra, A. *J. Mol. Struct.* **1975**, *26*, 57−68.
(22) Ams, M. R.; Ajami, D.; Craig, S. L.; Yang, J. S.; Rebek, J., Jr. *Beilstein J. Org. Chem.* **2009**, *5*, 79.
(23) Tzeli, D.; Theodorakopoulos, G.; Petsalakis, I. D.; Ajami, D.; Rebek, J., Jr. *J. Am. Chem. Soc.* **2012**, *134*, 4346−4354.
(24) Parise, J. B. *J. Inclus. Phenom. Mol.* **1995**, *21*, 79−112.
(25) Parise, J. B.; Hriljac, J. A.; Cox, D. E.; Corbin, D. R.; Ramamurthy, V. *J. Chem. Soc., Chem. Commun.* **1993**, *3*, 226−228.
(26) Mentzen, B. F. *J. Phys. Chem. C* **2007**, *111*, 18932−18941.
(27) Mentzen, B. F.; Bergeret, G.; Emerich, H.; Weber, H. P. *J. Phys. Chem. B* **2006**, *110*, 97−106.
(28) Olson, D. H.; Khosrovani, N.; Peters, A. W.; Toby, B. H. *J. Phys. Chem. B* **2000**, *104*, 4844−4848.
(29) Beerdsen, E.; Dubbeldam, D.; Smit, B.; Vlugt, T. J.; Calero, S. *J. Phys. Chem. B* **2003**, *107*, 12088−12093.
(30) Schneider, S.; Scharnagl, C.; Bug, R. *J. Phys. Chem.* **1992**, *96*, 9748−9759.
(31) Waldman, M.; Hagler, A. T. *J. Comput. Chem.* **1993**, *14*, 1077−1084.
(32) Sun, H. *J. Phys Chem B* **1998**, *102*, 7338−7364.
(33) Frisch, M. J.; Trucks, G. W.; Schlegel, H. B.; Scuseria, G. E.; Robb, M. A.; Cheeseman, J. R.; Montgomery, Jr., J. A.; Vreven, T.; Kudin, K. N.; Burant, J. C. et al. *Gaussian 03*, revision D.01; Gaussian, Inc.: Wallingford, CT, 2004.
(34) Jobic, H.; Ghosh, R. E.; Renouprez, A. *J. Chem. Phys.* **1981**, *75*, 4025−4030.
(35) Tomkinson, J.; Kearley, G. J. *J. Chem. Phys.* **1989**, *91*, 5164−5169.
(36) Tomkinson, J.; Kearley, G. J. *Nucl. Instrum. Methods Phys. Res., Sect. A* **1995**, *354*, 169−170.
(37) Smirnov, K. S.; Bougeard, D. *Zeolites* **1994**, *14*, 203−207.
(38) Van de Graaf, B.; Njo, S. L.; Smirnov, K. S. Introduction to Zeolite Modeling. In *Reviews in Computational Chemistry*; Lipkowitz, K. B., Boyd, D. B., Eds.; Wiley-VCH: New York, 2000; Vol. *14*, p 193.
(39) Obrzut, J.; Karasz, F. E. *J. Chem. Phys.* **1987**, *87*, 2349−58.
(40) Katoh, R.; Suzuki, K.; Furube, A.; Kotani, M.; Tokumaru, K. *J. Phys. Chem. C* **2009**, *113*, 2961−2965.
(41) Agbaria, R. A.; Roberts, E.; Warner, I. M. *J. Phys. Chem.* **1995**, *99*, 10056−10060.
(42) Meic, Z.; Gusten, H. *Spectrochim. Acta, Part A* **1978**, *34*, 101−111.
(43) Baranovic, G.; Meic, Z.; Gusten, H.; Mink, J.; Keresztury, G. *J. Phys. Chem.* **1990**, *94*, 2833−2843.
(44) Watanabe, H.; Okamoto, Y.; Furuya, K.; Sakamoto, A.; Tasumi, M. *J. Phys. Chem. A* **2002**, *106*, 3318−3324.
(45) Lercher, J. A.; Jentys, A. *Stud. Surf. Sci. Catal.* **2007**, *168*, 435−476.
(46) Delahay, G.; Guzman-Vargas, A.; Coq, B. *Appl. Catal., B* **2007**, *70*, 45−52.